Ab initio calculation of the stoichiometry and structure of the (0001) surfaces of GaN and AlN

Jürgen Fritsch, Otto F. Sankey, Kevin E. Schmidt, and John B. Page
Department of Physics and Astronomy, Arizona State University, Tempe, Arizona 85287-1504
(Received 19 June 1997)

We have investigated the stoichiometry and the atomic and electronic structure of the anion- and cation-terminated (0001) surfaces of wurtzite-phase GaN and AlN, using *ab initio* local-orbital calculations based on the local-density approximation and the pseudopotential method. All stable surface configurations studied differ in atomic composition and periodicity from the ideal bulklike termination. We compare the total energy computed for various $p(2\times2)$ geometries of GaN and AlN(0001). Vacancy structures are found to be the most stable configurations for the anion- and cation-terminated surfaces. For metal-rich growth conditions, our calculations favor the adsorption of metal atoms on the cation-terminated surface. Anion- and cation-derived dangling-bond states appear in the bulk band gap as a result of the formation of vacancies or the adsorption of group-III atoms. Flat surfaces of both types are found to be stabilized by a $\frac{3}{4}$ ML adsorption of hydrogen. [S0163-1829(98)05919-0]

I. INTRODUCTION

Thin GaN and AlN films are typically grown on the hexagonal surfaces of sapphire and 6*H*-SiC by means of molecular-beam epitaxy (MBE) or metal-organic chemical-vapor deposition (MOCVD).[1–5] Two of the most striking applications of heteroepitaxy on sapphire are the fabrication of blue-light-emitting *p-n* junctions[6] and the realization of laser diodes[7] using GaN. Recent developments aim to optimize the growth of group-III nitrides with the help of selected energy epitaxy.[8] Deposited on hexagonal substrates, the nitride films crystallize in the more stable wurtzite structure. Possible growth faces are the cation-terminated (0001) or the anion-terminated $(000\bar{1})$ surface.

Although many different experiments have been performed to monitor the epitaxial process and to characterize the resulting morphology of thin films, the growth front has not yet been understood completely. By means of low-energy electron diffraction (LEED) or reflection high-energy electron diffraction, sharp $p(1\times1)$ patterns have been reported for well-ordered hexagonal surfaces of wurtzite-phase GaN and AlN,[1,9,10] while some MBE-grown nitride films exhibit a $p(2\times2)$ reconstruction.[5,11,12] Other experiments give indications of other higher-order reconstructions, such as $p(2\times1)$, $p(2\times3)$, or $p(5\times5)$.[13] In a recent scanning-tunneling microscopy experiment, linear and oval defects have been reported for GaN(0001), and attributed to vacancies.[14]

Total-energy calculations based on density-functional theory (DFT) in the plane-wave pseudopotential approximation have been performed to investigate the surface atomic structure of the (0001) surfaces of the group-III nitrides. Buongiorno Nardelli, Rapcewicz, and Bernholc studied the cation- and anion-terminated (0001) surfaces of GaN, restricting their calculations to $p(2\times2)$ geometries.[15] For the cation-terminated surface, the adsorption of one gallium atom on the atop (T_4) site was found to be the most stable configuration under metal-rich conditions. The adsorption of one nitrogen atom on the hollow (H_3) site is more stable in nitrogen-rich environments. For the anion-terminated $(000\bar{1})$ surface, the formation of nitrogen vacancies is favorable, according to Ref. 15. As pointed out in the *ab initio* calculation of Ref. 16, the polarity matching between the SiC(0001) substrate and the deposited film is of fundamental importance for the termination of the growing nitride film. By studying one and two bilayers of AlN deposited on Si-terminated SiC(0001), Di Felice, Northrup, and Neugebauer concluded that the formation of Al-vacancy structures stabilizes thin AlN films with respect to island formation.[17] Nitrogen adatom structures were found to be unfavorable in Ref. 17. Calculations based on a tight-binding approach indicate that a silicon-terminated surface guarantees better lattice matching for GaN grown on 6*H*-SiC.[18] Beyond these investigations, further calculations for the structure of the (001) surfaces of cubic group-III nitrides have been performed.[19]

The large variety of experimental observations reported in Refs. 1,5,9–12, and 13 can be explained only partially by the results obtained from the *ab initio* calculations of Refs. 15–17. Previous theoretical investigations have not examined the influence of hydrogen on the growth phase, as observed by experiment.[1]

Here we present a systematic analysis of a large variety of possible surface structures for the hexagonal surfaces of wurtzite-phase GaN and AlN. We perform molecular-dynamics simulations using a fast *ab initio* multicenter local-orbital formalism.[20–23] This method has been successfully applied to the structural, electronic, and vibrational studies of many systems including fullerenes as well as free and adsorbate-covered surfaces.[23–26] Although the method is less computationally intensive compared to other *ab initio* schemes, we obtain good agreement with available experimental data and with self-consistent pseudopotential calculations, for lattice parameters,[27] phonon frequencies,[28,29] and the structure of the nonpolar surfaces of GaN and AlN.[30,31]

The efficiency of the method allows us to compute the relaxation and total energy of systems with a large number of atoms and for many different atomic arrangements. Besides the geometries discussed in Ref. 15 for GaN(0001), in our calculations we include additional configurations, such as a nitrogen-vacancy complex which is found to be more stable compared to the simple nitrogen vacancy. We also perform calculations for the adsorption of hydrogen, which stabilizes

the anion- and cation-terminated surfaces. In addition, we discuss the dispersion of the electronic surface states determined for the most stable surface reconstructions. In the absence of hydrogen, we find the $p(2\times2)$ nitrogen-vacancy complex to be the most stable structure for the anion-terminated surfaces of GaN and AlN. For the cation-terminated surface, the cation $p(2\times2)$ vacancy is the lowest-energy structure. Under metal-rich growth conditions, the adsorption of a metal atom in the atop (T_4) position is slightly more favorable. For all reconstructions, characteristic anion-derived dangling-bond states are found above or near the bulk valence band maximum, while cation-derived dangling-bond states appear in the upper half of the bulk band gap.

The paper is organized as follows: In Sec. II, we give a brief outline of the theoretical basis of our calculations. Section III illustrates the degree of accuracy of our computations by summarizing the results obtained for the bulk lattice parameters and phonon frequencies. In Sec. IV, we discuss various surface geometries considered for the anion- and cation-terminated (0001) surfaces of GaN and AlN. We compare the total energies of the most stable structures, and analyze atomic relaxations in detail. Surface electronic states of low-energy surface configurations are examined in Sec. V. Section VI summarizes our results and conclusions.

II. THEORETICAL METHOD

Our total-energy calculations are carried out by means of an *ab initio* multicenter tight-binding-like model which is based on the density-functional theory in the local-density approximation.[32–35] We employ norm-conserving pseudopotentials[36] to describe the electron-ion interaction. The electronic wave functions and charge density are represented by a superposition of pseudoatomic orbitals (PAO's) $\phi_i(\mathbf{r}-\mathbf{R}_i)$ using the valence electron s and p orbitals for N, Al, and Ga, and the $1s$ orbital for H. In particular, the total valence charge density is approximated by

$$n_{\rm in}(\mathbf{r})=\sum_i n_i|\phi_i(\mathbf{r}-\mathbf{R}_i)|^2, \tag{1}$$

which is used as the input charge density for the Harris functional approach[37] employed to compute the total energy.[20]

The determination of the lattice constant, the bulk modulus, and the optical-phonon frequencies of GaN and AlN shows that it is necessary to treat the group-III nitrides within the generalized scheme introduced in Ref. 22, which includes charge transfer between the ions in a self-consistent fashion. This is done by using variable occupation numbers n_i for the representation of the charge density [Eq. (1)]. The Kohn-Sham equations are solved iteratively, until convergency (in the sense of Ref. 22) is achieved for the occupation numbers n_i. For rapid convergence of the iterative procedure, we use the mixing scheme suggested in Ref. 38.

The PAO's are constructed using the boundary condition that they vanish beyond a specified cutoff radius r_c. This restricts the short-range interaction contributions to a small number of neighboring atoms. Due to the confinement, the PAO's are slightly excited, yielding slightly contracted atomic charge densities. Confined atomic orbitals significantly improve the accuracy of the Harris functional, since they simulate the contraction of the atomic charge density observed in solid-state systems.[39] The choice of the confinement radii r_c has to guarantee that the energy differences between the atomic levels of the free atoms ($r_c\rightarrow\infty$) is essentially the same as that of the contracted atoms. In our calculations, we use $r_c=5.4$ (in atomic units) for gallium, $r_c=5.4$ for aluminum, $r_c=3.8$ for nitrogen, and $r_c=3.7$ for hydrogen to compute all interaction terms and overlap integrals. The only deviation from these values is that we employ less confined PAO's for gallium ($r_c^{\rm coul}=5.7$), aluminum ($r_c^{\rm coul}=6.0$), and nitrogen ($r_c^{\rm coul}=3.95$) to compute the Coulomb integrals in the electron double-counting correction U_{ee} (see Ref. 20). This slightly increases the interatomic repulsion, and consequently the lattice constants determined for AlN and GaN.

Our surface calculations are carried out for systems of periodically repeated thin crystal films spanning five atomic double layers. We restrict our investigations to surface reconstructions with $p(2\times2)$ symmetry. The top layer of the slab supercell comprises only nitrogen atoms, while the bottom layer of the thin crystal film is composed of cations. In the case of ideal surfaces, the slab supercell contains 20 nitrogen atoms and 20 group-III atoms (gallium or aluminum), with one dangling bond for each top- and bottom-layer atom. Convergence tests performed for crystal films spanning nine atomic double layers show that five bilayers are sufficient to decouple the two individual surfaces of the slabs. The thickness of the vacuum region between neighboring crystal films is about 13 Å, which gives a negligible interaction between neighboring slabs. The dimensions of the slab supercells are chosen in accordance with the lattice constants a and c and the internal parameter u, all determined from the bulk phase of the wurtzite compounds. For the **k**-point sampling we use eight special points according to a two-dimensional 8×8 Monkhorst-Pack grid[40] in the surface Brillouin zone of the $p(2\times2)$ unit cell.

In order to find the atomic positions of minimal energy for a given configuration, we perform molecular-dynamics simulations by determining the Hellmann-Feynman forces, and move the atoms according to the classical equations of motion. The atomic masses of the central bilayer are increased to essentially infinity, leading to frozen atomic positions in the central part of the slab supercell. All other atoms in the crystal films are allowed to move. The atomic positions of minimal energy are determined by systematically reducing the kinetic energy of the system (''power'' quenching). In this scheme, the velocity component $v_{i\alpha}$ of the ith particle is set to zero whenever $v_{i\alpha}F_{i\alpha}<0$, where $F_{i\alpha}$ is the Hellmann-Feynman force acting on the particle in the direction α. For power quenching, we use a time step of 2.5 fs. For all configurations, the minimization converged satisfactorily after 100 time steps with an uncertainty in the computed atomic positions of less than 0.02 Å.

III. BULK PROPERTIES

An important prerequisite for the investigation of the (0001) surfaces is to calculate the bulk properties of GaN and AlN, especially for the wurtzite phase, with sufficient accuracy. This is essential since the lattice parameters obtained

TABLE I. Structural parameters a, c, and u, bulk modulus B_0, and Γ-point frequency (in cm^{-1}) of the optical modes of GaN and AlN in the wurtzite structure. Columns 4 and 7: results of the mixed-basis calculation of Miwa and Fukumoto (Ref. 29).

	Wurtzite GaN			Wurtzite AlN		
	Present work	Experiment	DFT Miwa and Fukumoto	Present work	Experiment	DFT Miwa and Fukumoto
a (Å)	3.088	3.190[a]	3.146	3.070	3.110[a]	3.144
c (Å)	5.041	5.189[a]	5.125	4.937	4.980[a]	5.046
u	0.376	0.377[a]	0.377	0.381	0.382[a]	0.381
B_0 (MBar)	2.09	–	1.95	2.56	2.02[b]	1.95
E_2^1	190	144[c]	146	330	241[c]	228
B_1^1	329	–	335	540	–	534
A_1-TO	538	537[d]	534	626	614[e]	601
E_2^2	566	571[d]	568	642	660[e]	655
E_1-TO	563	556[d]	556	665	673[e]	650
B_1^2	715	–	697	746	–	703

[a]Reference 41.
[b]Reference 42.
[c]Reference 43.
[d]Reference 44.
[e]Reference 45.

for the bulk define the dimensions of the slab supercells used in the computation of the surface properties. Wurtzite-phase compound semiconductors are characterized by three independent structural parameters, namely, the in-plane lattice constant a, the lattice constant c along the hexagonal axis, and the internal parameter $u=d/c$, which reflects the length d of the anion-cation bond along the c axis.

The total-energy calculations for wurtzite-compound GaN and AlN have been carried out using 12 special points in the three-dimensional Brillouin zone of the bulk, using an $8\times8\times8$ Monkhorst-Pack grid[40] for the **k**-point sampling. For a given pair of a and c, the atomic positions of the four atoms in the bulk unit cell are relaxed along the c axis with respect to the Hellmann-Feynman forces. For each pair (a,c), we obtain an optimized value for the internal parameter $u_{\mathrm{opt}}(a,c)$ which minimizes the total energy $E_{\mathrm{tot}}[a,c;u_{\mathrm{opt}}(a,c)]$. The optimization of u is repeated on a grid of 36 pairs (a,c) defined by the combination of six different values of a and c chosen in a narrow interval about the experimentally measured data. By fitting the 36 energy values $E_{\mathrm{tot}}[a,c;u_{\mathrm{opt}}(a,c)]$ to a cubic equation in the cell volume V and the ratio c/a in analogy to Ref. 27, we find the equilibrium values for the lattice parameters a, c, and u.

Our results obtained for wurtzite-phase GaN and AlN are summarized in Table I, together with the bulk modulus B_0 and the optical zone-center phonon frequencies. The comparison with the experimental data of Refs. 41–45 and the *ab initio* calculation of Miwa and Fukumoto[29] shows an overall good agreement, with a small underestimation of the lattice constants by about 3% for GaN and 1% for AlN. Similar agreement is achieved for the Γ-point phonon frequencies, which we have determined by means of the frozen-phonon approach. However, the frequency of the E_2^1 mode, which consists of an out-of-phase vibration of neighboring bilayers polarized in the hexagonal plane (see Fig. 1 of Ref. 28), is significantly overestimated by our calculation.

For zinc-blende GaN, we obtain a value of 4.382 Å for the lattice constant, which is about 3% smaller than the experimental result of 4.519 Å.[3] The frequency computed for the TO-phonon mode amounts to 541 cm^{-1}, which is close to the value 555 cm^{-1} measured by Raman spectroscopy.[44] The corresponding lattice constant and TO-phonon frequency calculated for AlN are 4.342 Å and 643 cm^{-1}. Because of the lack of experimental data for zinc-blende-phase AlN, we compare our results to the mixed-basis approach of Ref. 29, which yields 4.421 Å and 648 cm^{-1}, respectively.

Since the Ga $3d$ state is not included in the minimal-basis local-orbital formalism, we obtain a slight underestimation of the structural parameters calculated for GaN. The differences from the experimental data are only marginal for AlN. Hence our results agree with measured values about as well as those obtained from the highly converged pseudopotential calculations of Refs. 27–29. In addition, we also achieve good agreement with the findings of other *ab initio* calculations obtained for the structure of the nonpolar surfaces of GaN and AlN,[30,31] including the relaxation, surface energy, and energy differences determined for various surface stoichiometries. This is of fundamental importance for the investigation of the reconstructions and stoichiometry of the (0001) surfaces of GaN and AlN and their dependence on the chemical potentials of the bonding partners.

IV. SURFACE STRUCTURES

The polarity of GaN and AlN has an important influence on the structure of the surfaces of these materials. Atomically flat surfaces and interfaces with (0001) orientation would lead to a macroscopic electric field.[46–48] Processes that eliminate the surface polarity and the associated electric field are

based on two primary concepts: chemical bonding and autocompensation.[47] Autocompensation consists of a charge transfer from the dangling bonds of the more electropositive element to the more electronegative element, which guarantees that the anion-derived surface dangling bonds are completely occupied, while the cation-derived dangling bonds are empty.

For the hexagonal surfaces of GaN and AlN, it is necessary to modify the surface stoichiometry in order to achieve autocompensation and to eliminate the surface polarity. This has been demonstrated in Harrison's electron-counting model[48] for the (111) surfaces of III-V semiconductors, which are the zinc-blende-compound analogs to the hexagonal surfaces of wurtzite-phase GaN and AlN. Among the zinc-blende compounds, well-known examples are GaAs, InAs, and InSb. The cation- and anion-terminated surfaces of these materials are known to form $p(2\times2)$ reconstructions with the cation (111) $p(2\times2)$ surfaces exhibiting a cation vacancy,[49,50] while the anion $(\overline{111})$p(2×2) surfaces are stabilized by the adsorption of anion trimers.[51,52] For GaN and AlN, similar modifications of the surface stoichiometry, including the formation of vacancies or the adsorption of atoms, are expected to compensate for the polarity, and hence to stabilize the hexagonal surfaces.

To compare the total energies computed for different atomic compositions of the cation-terminated (0001) and anion-terminated $(000\overline{1})$ surfaces, the chemical potentials μ_{Ga}, μ_{Al}, and μ_{N} of gallium, aluminum, and nitrogen have to be taken into account, in analogy with Ref. 53. We assume equilibrium with the bulk material, so that the chemical potentials of the bonding partners are related by

$$\mu_{\mathrm{Ga}}+\mu_{\mathrm{N}}=\mu_{\mathrm{GaN(bulk)}} \tag{2}$$

in the case of GaN, and

$$\mu_{\mathrm{Al}}+\mu_{\mathrm{N}}=\mu_{\mathrm{AlN(bulk)}} \tag{3}$$

for AlN. The chemical potentials $\mu_{\mathrm{GaN(bulk)}}$ and $\mu_{\mathrm{AlN(bulk)}}$ are the total energies per anion-cation pair computed for the wurtzite-phase compounds at zero temperature. We obtain $\mu_{\mathrm{GaN(bulk)}}=-337.024$ eV and $\mu_{\mathrm{AlN(bulk)}}=-331.755$ eV. Equations (2) and (3) allow us to calculate surface energies as a function of only the chemical potential of the respective metal atom, which is restricted to

$$\mu_{\mathrm{metal(bulk)}}-\Delta\mu\leqslant\mu_{\mathrm{metal}}\leqslant\mu_{\mathrm{metal(bulk)}}\,. \tag{4}$$

In cation-rich conditions, the metal chemical potentials are $\mu_{\mathrm{Ga(bulk)}}=-59.57$ eV and $\mu_{\mathrm{Al(bulk)}}=-53.60$ eV, determined for metallic α-gallium and aluminum. The range $\Delta\mu$ for the chemical potentials is the same as that of Refs. 17 and 54. In our surface calculations, we use slab supercells with anion termination on the upper surface and cation termination on the opposite side. The two individual surfaces of the crystal films are independent. For each of the individual surfaces, we consider the various surface geometries that are illustrated in Figs. 1 and 2.

We consider reconstructions with $p(2\times2)$ symmetry exclusively. In the vacancy model, one of the four first-layer atoms per unit cell is missing. This generates one dangling bond for each of the three second-layer atoms that are next to the vacancy. The lower part of Fig. 1 illustrates the vacancy

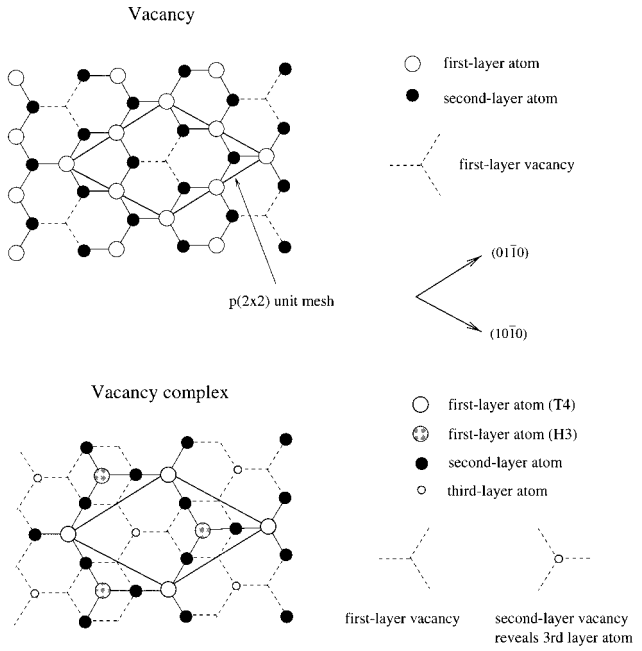

FIG. 1. Schematic top view of the vacancy and the vacancy complex. The atomic positions of the first two layers (three layers for the vacancy complex) are displayed. Open and closed circles represent first- and second-layer atoms. For anion termination, the white and black circles correspond to nitrogen and group-III atoms, respectively. For the case of a cation-terminated surface, the open and closed circles illustrate first-layer group-III atoms and second-layer nitrogen. The $p(2\times2)$ unit cell used in all calculations is indicated.

complex originally suggested in Refs. 55 and 56 for the GaAs$(\overline{111})$ surface. One out of four second-layer atoms per unit cell is missing in this structure. As indicated by the small open circles, the removal of second-layer atoms reveals third-layer atoms which are located directly below the second layer. Only two out of four first-layer atoms per unit cell are present in the vacancy complex. One of the two atoms resides on the regular T_4 (atop) position which corresponds to the corners of the $p(2\times2)$ unit mesh indicated in Fig. 1. The other first-layer atom per unit cell is moved from a T_4 to the H_3 (hollow) site. This results in the creation of a planar sp^2-like bonding configuration for the second-layer atoms, which have two first-layer and one third-layer nearest neighbors.

In addition to the atom deficiency structures illustrated in Fig. 1, we consider $p(2\times2)$ adsorption geometries as shown in Fig. 2. In the H_3 (hollow) adsorption site, the chemisorbed atoms are bonded to three first-layer atoms residing in positions above the surface between first- and second-layer atoms. In the T_4 (atop) site, the adsorbed atoms are bonded to three first-layer atoms in positions directly above second-layer atoms. We investigate the chemisorption of group-III atoms as well as the adsorption of nitrogen on H_3 and T_4 positions.

All of these surface reconstructions are studied for both anion- and cation-terminated surfaces of GaN and AlN. We also consider the adsorption of hydrogen on the cation- and anion-terminated surfaces. A recent experiment using time-of flight scattering and recoiling spectrometry, provides

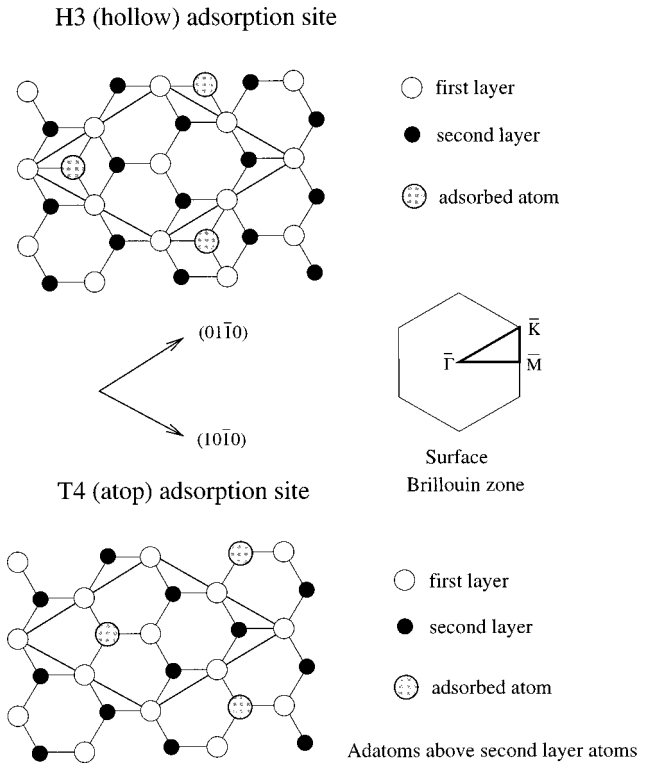

FIG. 2. Top view of the adsorption geometries considered within the $p(2\times2)$ reconstruction model. In the H_3 (hollow) adsorption site, the chemisorbed atoms are bonded to three first-layer atoms residing positions between first- and second-layer atoms. In the T_4 (atop) site, the adsorbed atoms are bonded to three first-layer atoms in positions directly above second-layer atoms. Also indicated is the two-dimensional Brillouin zone of the $p(2\times2)$ reconstructed surface and its irreducible wedge, indicated by the heavy lines.

evidence for a 75% coverage of the flat GaN$(000\bar{1})$ surface with hydrogen.[1] Figure 3 illustrates the adsorption model proposed according to the experimental results. A $p(2\times2)$ reconstruction is assumed, with $\frac{3}{4}$ ML of hydrogen saturating the dangling bonds of three out of four surface atoms per unit cell.

A particular surface reconstruction fixed on one side of the slab supercell might be used as a reference configuration

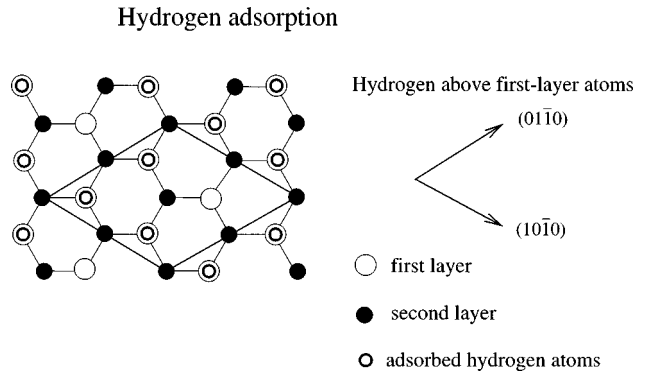

FIG. 3. Top view of the $\frac{3}{4}$-ML $p(2\times2)$ hydrogen adsorption model proposed by Sung *et al.* (Ref. 1). The dangling bonds of three out of four surface atoms per unit cell are saturated by hydrogen.

to compare various geometries on the other surface of the crystal films. To investigate to what extent the two individual surfaces of the slabs are decoupled, we performed calculations for a large variety of systems in which we combined all of the above-mentioned surface structures assumed for the nitrogen-terminated side with many different geometries taken into consideration for the cation-terminated side. For AlN(0001), we have determined the relaxed atomic positions and the total energy for over 30 different combinations. The total energies comprise the effects of both surfaces of the slab supercell and also reflect to what extent the two surfaces interact. One important result is that the energy differences between the structures examined for one side of the crystal film are essentially independent of the reference configuration chosen on the other side of the thin slab. This shows that the bottom and top layers of the crystal films are sufficiently decoupled. We have also checked this by using crystal films spanning nine bilayers.

Also, the surface electronic states are essentially the same for a given reconstruction, assuming different reference configurations on the other side of the slab. Although our supercells contain two different surfaces, occupied surface states on one side of the film are normally lower in energy than empty states on the opposing surface. This is related to the fact that occupied band-gap states (originating from chemical bonds and nitrogen-derived dangling bonds) are close to the valence-band maximum in most of the cases, while empty surface states (stemming from cation-derived dangling bonds) are generally near the conduction-band edge. In addition, all surface structures considered here are in accord with the autocompensation principle. Hence most of the slab geometries we have investigated are semiconducting. Atomic relaxations normally decrease the energy of occupied band-gap states, while empty surface states are shifted to a higher energy. In particular, the lowest-energy structures are characterized by a clear gap between occupied and empty surface states. Because of this, eight special points such as used in our computations are sufficient for a well-converged **k**-point sampling.

To compare the surface energies for different stoichiometries, the total number of cations (n_{Ga} or n_{Al}) and anions (n_{N}) in the slab supercell has to be taken into account. For a given combination of atomic geometries on the upper and lower surfaces of the thin film, the surface energy per $p(2\times2)$ unit cell is equal to

$$E_{\mathrm{surf}}=E_{\mathrm{tot}}-n_{\mathrm{Ga}}\mu_{\mathrm{Ga}}-n_{\mathrm{N}}(\mu_{\mathrm{GaN(bulk)}}-\mu_{\mathrm{Ga}}) \qquad (5)$$

for GaN, and analogously for AlN. The energy E_{tot} is the total energy per slab supercell, determined for completely relaxed positions on both sides of the slab. The chemical potentials vary in a range according to Eq. (4), leading to a variation of the calculated surface energy if the number of group-III atoms is different than the number of nitrogen atoms.

A. Cation-terminated surface

We summarize our results for the cation-terminated surface of GaN and AlN obtained with the nitrogen-vacancy complex as the reference configuration on the $(000\bar{1})$ surface. Figure 4 displays the surface energies per $p(2\times2)$ unit

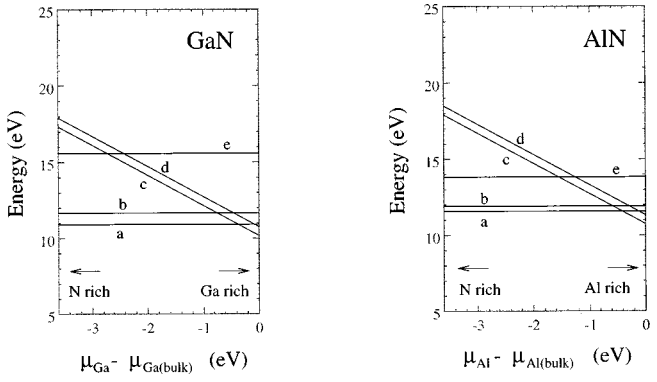

FIG. 4. Total energies per $p(2\times2)$ unit cell for various surface reconstructions of the cation-terminated GaN and AlN(0001) surface. The nitrogen-vacancy complex on the anion-terminated side has been chosen as the reference configuration. The labels symbolize the following geometries: (a) vacancy, (b) adsorption of nitrogen on the H_3 site, (c) adsorption of a group-III atom on the T_4 site, (d) adsorption of a group-III atom on the H_3 site, and (e) adsorption of nitrogen on the T_4 site.

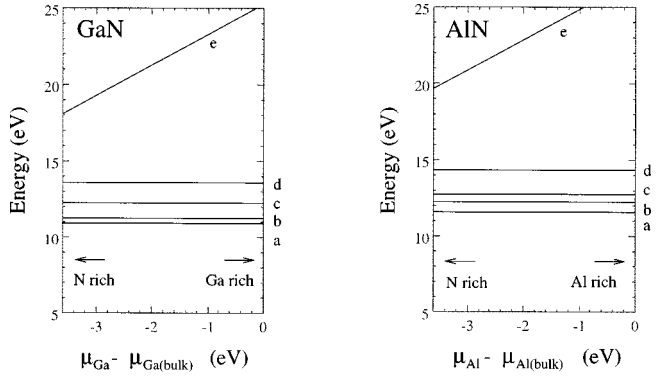

FIG. 5. Total energies per $p(2\times2)$ unit cell for various surface reconstructions of the anion-terminated GaN and AlN$(000\bar{1})$ surface. The cation vacancy on the cation-terminated side has been chosen as the reference configuration. The labels symbolize the following geometries: (a) vacancy complex, (b) vacancy, (c) adsorption of a group-III atom on the H_3 site, (d) adsorption of a group-III atom on the T_4 site, and (e) adsorption of nitrogen on the T_4 site.

cell determined for the most important reconstructions. The lowest-energy configuration is the cation-vacancy arrangement labeled (a), which is lower by about 0.7 eV (0.3 eV) than the configuration with adsorbed nitrogen on the hollow site (b) of the (0001) surface of GaN (AlN). For the chemisorption of nitrogen, the H_3 site (b) is preferred above the T_4 position (e) by 4.0 eV (1.9 eV) in the case of GaN (AlN). The adsorption of a nitrogen atom changes the stoichiometry in the same way as the creation of a cation vacancy, since in both cases the number of cations in the surface bilayer is one less than the number of anions. Consequently, the relative energy difference of the structures (a), (b), and (e) is independent of the chemical potential of the group-III atoms. In contrast to this, the adsorption of group-III atoms involves more cations than anions in the surface region, leading to relative energies that depend on the chemical potential of the metal atoms as compared to structures (a), (b), and (e). Hence the metal-adatom T_4 configuration (c) is lower in energy than all other structures in a range of $-0.4\text{eV} \leqslant \Delta\mu \leqslant 0.0$ eV(-0.45 eV$\leqslant\Delta\mu\leqslant 0.0$ eV) for the chemical potential of gallium (aluminum). The H_3 adsorption site (d) is less favorable by 0.6 eV for both compounds. This agrees very well with the *ab initio* calculation of Ref. 15, which obtained the lowest energy for the adsorption of group-III atoms on the T_4 site of GaN(0001) in metal-rich conditions. In contrast with Ref. 15 but in agreement with the *ab initio* study of Ref. 17, our calculation slightly favors the cation vacancy over the adsorption of nitrogen on the hollow site.

Among all different geometries having cation deficiency, including the vacancy complex and the staggered vacancy as introduced by Kaxiras *et al.* for GaAs$(\bar{1}\bar{1}\bar{1})$,[56] the vacancy configuration has the lowest energy. The atomic relaxations associated with the removal of one out of four surface atoms result in a nearly planar bonding configuration of those second-layer nitrogen atoms [one per $p(2\times2)$ unit cell], which are bonded to all three remaining first-layer atoms. Compared with the ideal positions, the first-layer atoms are shifted downward by about 0.18 Å (0.02 Å) in GaN(0001) [AlN(0001)], and the nitrogen atoms bonded to three first-layer atoms are raised by about 0.32 Å (0.55 Å). The three other second-layer atoms, which are closest to the vacancy, are raised only slightly by about 0.08 Å (0.15 Å), and show only small in-plane relaxations, directed away from the vacancy.

Among all investigated configurations with one additional atom per $p(2\times2)$ unit cell (including on top adsorption and atomic exchange), we find that the chemisorption of nitrogen on the H_3 position and the adsorption of a group-III atom on the T_4 site under metal-rich conditions give the most stable structures. The adsorption of a metal atom on the T_4 position of the GaN(0001) [AlN(0001)] surface induces a slight upward relaxation of the first-layer atoms involved in the chemisorption, by about 0.13 Å (0.25 Å). No other significant relaxations occur. The adsorbed layer is 1.78 Å (1.95 Å) above the outermost cation plane, the bond lengths amount to 2.50 Å for the Ga-Ga bonds and 2.60 Å for the Al-Al bonds. For the case of nitrogen adsorption on the hollow site of GaN(0001) [AlN(0001)], the three first-layer cations bonded to nitrogen are raised upward by about 0.19 Å (0.38 Å), leading to a vertical separation between the nitrogen and its bonding partners of 1.17 Å (1.19 Å). In-plane relaxation toward the adsorbed nitrogen with a magnitude of 0.19 Å (0.18 Å) occurs, reducing the cation-nitrogen bond length to 1.96 Å (1.99 Å). The fourth first-layer atom not involved in the chemical bond is shifted downward by 0.37 Å (0.15 Å).

B. Anion-terminated surface

For the different structures considered on the anion-terminated GaN$(000\bar{1})$ and AlN$(000\bar{1})$ surface, we summarize our results obtained with the cation vacancy as the reference configuration on the cation-terminated side of the slab supercells. Figure 5 displays the energies for the nitrogen-vacancy complex (a), the nitrogen vacancy (b), the adsorption of a group-III atom on the H_3 (c) and the T_4 (d) sites, as well as the adsorption of nitrogen on the T_4 position (e). The structures in Figs. (a)–(d) are similar in stoichiometry, with one nitrogen atom less per $p(2\times2)$ unit cell compared to the

number of cations in the surface region. For both compounds, the energy order of the different structures is the same. In agreement with Ref. 15, the nitrogen vacancy is found to be more stable compared with adatom configurations.

However, our calculation shows that the vacancy complex of Fig. 1, which has not been considered in previous calculations, is even lower in energy. Particularly for AlN$(000\bar{1})$, the vacancy complex turns out to be more stable by 0.7 eV than the vacancy, while the energy difference is slightly smaller for the case of GaN$(000\bar{1})$, for which we find the vacancy complex to be more stable by 0.3 eV. No significant atomic relaxations occur in the nitrogen-vacancy complex of GaN and AlN$(000\bar{1})$. Clear atomic shifts are seen only for AlN, for which we obtain an outward relaxation of the first-layer atoms by about 0.17 Å. Compared to this, larger relaxations are prominent in the nitrogen-vacancy geometry that is characterized by only a single missing first-layer nitrogen atom per unit cell. In GaN$(000\bar{1})$, the nitrogen vacancy exhibits essentially atomic in-plane shifts of the second-layer gallium atoms, increasing the distance to the vacancy by 0.23 Å. In AlN$(000\bar{1})$, the first bilayer is raised by about 0.13 Å and there is an additional upward relaxation of the fourfold bonded second-layer aluminum atoms by 0.11 Å. The other aluminum atoms relax away from the vacancy by about 0.18 Å.

The most stable adatom configuration of GaN$(000\bar{1})$ [AlN$(000\bar{1})$] involves the chemisorption of a group-III atom on the H_3 position. In this case, the first-layer nitrogen atoms are raised by 0.17 Å (0.36 Å), and show an in-plane relaxation toward the adsorbed atom by about 0.12 Å (0.13 Å). The chemisorbed atoms are 0.83 Å (0.86 Å) above their first-layer bonding partners, with a bond length of 1.86 Å (1.85 Å).

The adsorption of a group-III atom at positions other than the H_3 site, such as the T_4 site or on top of surface atoms, leads to significantly higher energies. Surface stoichiometries with anion excess, such as those formed by the adsorption of nitrogen, can be excluded. This is clear from Fig. 5, which shows that the most favorable adsorption site for nitrogen, the T_4 position, is higher in energy by at least 5 eV compared to all other structures. In contrast with the $(\bar{1}\bar{1}\bar{1})$ surfaces of III-V compounds like GaAs or GaSb, the adsorption of anion trimers is found to be unfavorable on the $(000\bar{1})$ surfaces of GaN and AlN. Because of their chemical nature, nitrogen atoms do not have the tendency to form trimers, while the heavier group-V atoms As and Sb are known to easily form trimers or clusters. Finally, we have considered additional surface reconstructions, such as the ''puckered hexagon'' and tetramers which were suggested in Ref. 56 for GaAs$(\bar{1}\bar{1}\bar{1})$. All of these surface reconstructions are found to be higher in energy compared with the vacancy, the vacancy complex, and the adsorption of group-III atoms on the H_3 position.

C. Surface structures in the presence of hydrogen

In the discussion of possible surface geometries, so far only structures that contain exclusively group-III atoms and nitrogen have been considered. Such conditions might be realized in molecular-beam epitaxy, in contrast with MOCVD, where a significant amount of hydrogen is present. For MOCVD-grown GaN films, Sung *et al.*[1] reported that cycles of sputtering and annealing in ultrahigh vacuum produce clean stoichiometric surfaces which yield sharp $p(1\times1)$ patterns in LEED. The time-of flight scattering and recoiling spectra recorded in Ref. 1 show the presence of hydrogen whenever a sharp $p(1\times1)$ LEED pattern is observed. To examine the extent to which hydrogen stabilizes the nitrogen-terminated surfaces, we compute the total energy for a free ammonia molecule above the $(000\bar{1})$ surface of GaN and AlN, with one nitrogen vacancy per $p(2\times2)$ unit cell. The result is compared to the case where the nitrogen atom of the molecule is incorporated into the vacancy, while the hydrogen atoms saturate three of the four dangling bonds (see Fig. 3). This structure corresponds to the adsorption of $\frac{3}{4}$ ML of hydrogen, as suggested in Ref. 1.

Our total-energy calculation shows that the adsorption system is lower in energy by 5.1 eV for GaN, and 5.4 eV for AlN. Hence the incorporation of ammonia into the nitrogen terminated surface is highly exothermic. The atomic relaxations in the hydrogen-terminated surface are smaller than 0.05 Å for GaN and AlN$(000\bar{1})$. For both compounds, we obtain a hydrogen-nitrogen bond length of 1.11 Å. The stability of the $\frac{3}{4}$-ML coverage is a consequence of the autocompensation principle. In a simplified picture, each nitrogen atom donates $\frac{5}{4}$ electrons to each bond, while each group-III atom contributes $\frac{3}{4}$ of an electron. Therefore, the nitrogen dangling bonds contain $\frac{5}{4}$ electronic charges. The adsorption of three hydrogen atoms per $p(2\times2)$ unit cell saturates the dangling bonds of the adsorption sites through the chemical bond, and saturates the fourth dangling bond of the ''lonely'' nitrogen atom through the excess charge resulting from the chemisorption.

Similar arguments hold for all of the other structures discussed in the previous subsections for the anion-and cation-terminated surfaces of GaN and AlN. In each case, the dangling bonds of surface anions are doubly occupied, while the dangling bonds of surface cations are empty. In particular, autocompensation can also be achieved by hydrogen adsorption on the cation-terminated surfaces. A coverage with $\frac{3}{4}$ ML of hydrogen results in the formation of three hydrogen-cation bonds (with a total of six electrons) and one empty cation dangling bond. The total energy of the $\frac{3}{4}$-ML adsorption geometry can be compared to a system that has free ammonia molecules above a surface composed of $p(2\times2)$ domains with cation vacancies and equal-size $p(2\times2)$ regions with metal adatoms. The decomposition of ammonia and the subsequent adsorption of the hydrogen and nitrogen atoms leads to a two-domain structure which contains regions with the $\frac{3}{4}$-ML hydrogen coverage and areas with $\frac{1}{4}$-ML nitrogen coverage, respectively. The energy gain for this process is 4.5 and 8.0 eV per $p(2\times2)$ unit cell for GaN and AlN. The bond lengths are 1.59 Å for the hydrogen-gallium bond, and 1.63 Å for the hydrogen-aluminum bond.

Since the charge distribution in the dangling bonds of a polar surface is sensitively dependent on the particular surface geometry and the existence of adsorbed atoms, the presence of hydrogen during epitaxy has an important influence

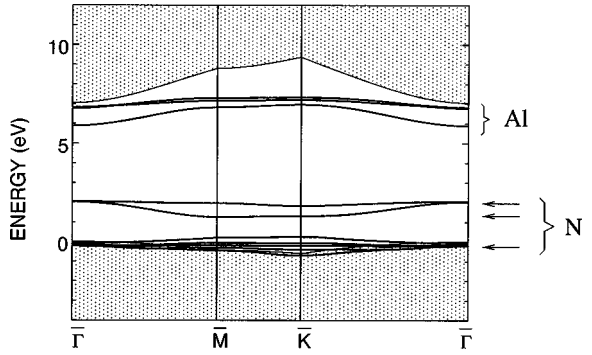

FIG. 6. Electronic dispersion for the AlN(0001) $p(2\times2)$ vacancy structure appearing in the bulk band gap. Surface localized states are indicated by solid lines. The large shaded areas represent the surface projected bulk band structure. The valence band maximum is at 0 eV.

on the growth of the hexagonal surfaces of AlN and GaN. For both cation- and anion-terminated surfaces, a $\frac{3}{4}$-ML coverage of hydrogen guarantees complete autocompensation with anion dangling bonds doubly occupied and cation dangling bonds empty. Therefore, chemisorption of hydrogen and nitrogen, followed by the decomposition of ammonia, leads to stable surface structures which are significantly lower in total energy for both kinds of termination compared with the hydrogen-free cases summarized in Figs. 4 and 5.

V. ELECTRONIC SURFACE STATES

As illustrated by Figs. 4 and 5, the hexagonal surfaces of AlN and GaN are similar with respect to the energetic order of the most important reconstructions. Moreover, the structural details of the atomic relaxation are essentially the same in each case. Because of this, the electronic surface states for a given reconstruction are similar for the two compounds. Here we restrict our discussion to AlN. We analyze the dispersion of the electronic surface states of the most stable reconstructions determined for the anion- and cation-terminated (0001) surface. All structures satisfy the principle of autocompensation, which requires that the cation-derived dangling bonds of a surface are empty, while the anion-derived dangling bonds are doubly occupied. Electronic surface states related to the dangling bonds and to the back-bonds of first-layer atoms and atoms next to vacancies

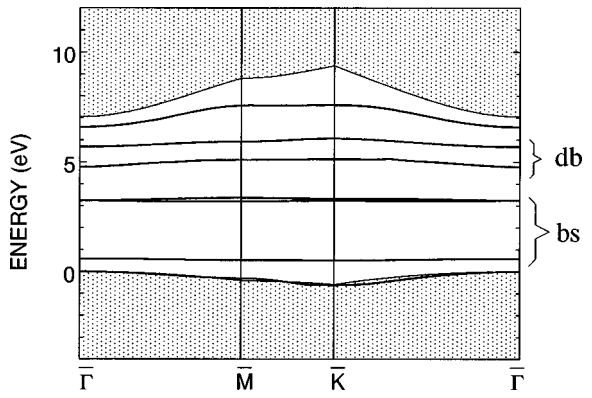

FIG. 7. Same as Fig. 6, but for the electronic dispersion of the aluminum T_4-adatom configuration in AlN(0001) $p(2\times2)$.

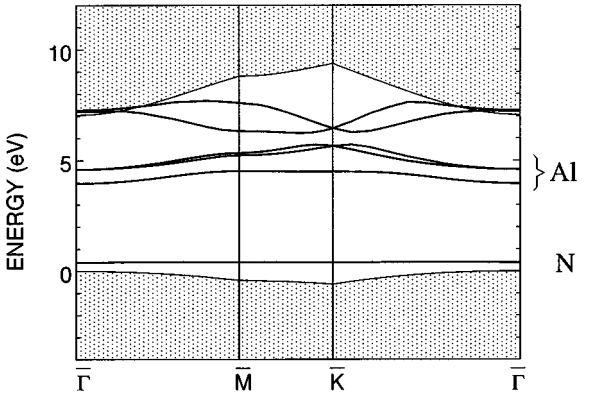

FIG. 8. Same as Fig. 6, but for the electronic dispersion of the AlN($000\bar{1}$) $p(2\times2)$ vacancy complex.

appear in the energy range of the bulk band gap. Figures 6–9 display all states appearing in the gap. With the principle of autocompensation in mind, we focus the discussion on surface states derived from dangling bonds. In contrast with plane-wave local-density-apporximation calculations that underestimate the band gap, our calculation overestimates the measured value of 6.3 eV (Ref. 3) for the bulk band gap of AlN by about 0.7 eV because of the small number of atomic orbitals used to describe the electronic wave functions.

A. Cation-terminated surface

The most stable configurations obtained for the cation-terminated AlN(0001) surface in the absence of hydrogen are the vacancy and adsorption of an aluminum atom on the T_4 site in metal-rich conditions. As seen from Fig. 1, the creation of one cation vacancy per $p(2\times2)$ unit cell leads to second-layer nitrogen atoms with three broken bonds oriented toward the missing first-layer atom. In addition, each of the three remaining surface atoms has one dangling bond in the direction of the surface normal. The band structure displayed in Fig. 6 exhibits three branches (indicated by Al) according to the cation-derived dangling bonds of the AlN(0001) vacancy structure. In analogy to the results obtained in Ref. 31 for the nonpolar $(11\bar{2}0)$ surface, these states appear above the Fermi level slightly below the bulk conduction band. Also in agreement with Ref. 31, nitrogen-derived dangling-bond states are found below the Fermi en-

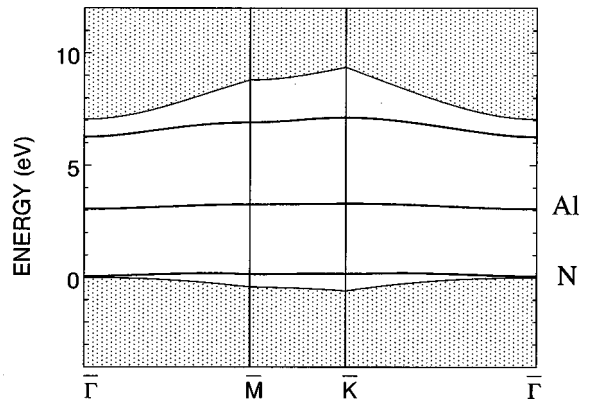

FIG. 9. Same as Fig. 6, but for the electronic dispersion of the aluminum H_3-adatom configuration in AlN($000\bar{1}$) $p(2\times2)$.

ergy close to the valence-band edge (indicated by N). In the vacancy structure, the dangling bonds of the three neighboring nitrogen atoms point to the position of the missing atom, and interact with each other. As a consequence, two nitrogen dangling-bond states are lifted by about 2 eV above the valence-band edge, while the third nitrogen dangling-bond state has an energy of about zero, with nearly no dispersion.

From Fig. 2, it can be seen that the adsorption of one aluminum atom per $p(2\times2)$ unit cell on a T_4 position leads to three Al-Al bonds. In the electronic band structure displayed in Fig. 7, three corresponding branches (labeled by bs) are prominent in the bulk band gap below the Fermi energy. Similar to the nitrogen dangling bonds of the vacancy, one lower-lying state with an energy of about 0.7 eV above the valence-band edge appears, together with two nearly degenerate branches at about 3.2 eV. While the state at 0.7 eV is mainly *s* like about the adsorbed atom, the pair of nearly degenerate branches primarily corresponds to the dangling bonds of the three surface atoms beneath the adsorbed aluminum. The two bands appearing in the gap at about 5 and 6 eV originate in the empty dangling bonds of the adsorbed atom and the surface atoms that are not involved in the chemisorption.

In the $\frac{3}{4}$-ML $p(2\times2)$ hydrogen adsorption system, four flat branches appear in the bulk band gap. Three nearly degenerate hydrogen-aluminum bonding states are prominent, with an energy of about 1 eV above the valence bands. The dangling bonds of the uncovered aluminum atoms are empty, and appear in the form of a nearly dispersionless band at about 6 eV, similar to the corresponding state shown in Fig. 7.

B. Anion-terminated surface

For the nitrogen-terminated AlN$(000\bar{1})$ surface, the vacancy, vacancy complex (Fig. 1), and adsorption of aluminum on the H_3 position are the lowest energy structures in the absence of hydrogen. Figure 1 illustrates that each second-layer aluminum atom in the vacancy complex is bonded in a planar sp^2-like configuration to one third-layer nitrogen atom directly underneath and to the pair of nearest nitrogen atoms in the top layer. Hence the dangling bonds of the three second-layer atoms per $p(2\times2)$ unit cell are *p* like and oriented perpendicular to the plane of the sp^2 orbitals which form the bonds to the nearest-neighbor nitrogen atoms. In the electronic dispersion of the nitrogen-vacancy complex shown in Fig. 8, three branches (indicated by Al) related to these dangling bonds occur above the Fermi level with an energy between 4 and 6 meV. Three more dangling bonds per $p(2\times2)$ unit cell are prominent in the vacancy complex. Besides the first-layer atoms, every fourth third-layer atom has a broken bond oriented perpendicular to the surface because of the formation of second-layer vacancies. While the dangling bonds of the first-layer atoms are lower in energy compared to the valence-band edge, the broken bond of the third-layer nitrogen atom can be recognized in the electronic band structure by a nearly dispersionless branch (labeled N in Fig. 8) at about 0.8 eV. The increase in energy reflects the larger Coulomb repulsion for the electrons occupying this dangling bond. These electrons are closer to the charge density of the surface. A series of additional surface-localized states related to the open structure of the vacancy-complex model appears slightly below the bulk conduction-band minimum.

For a first-layer nitrogen vacancy, three cation dangling-bond states are present in an energy range similar to that indicated by (Al) in Fig. 8. These bands are related to the second-layer atoms which are next to the missing nitrogen atoms. Compared to the vacancy complex, the dispersion of these states is larger. The first-layer nitrogen dangling bonds are found in the spectrum close to the valence-band maximum.

The adsorption of an aluminum atom at a hollow site on the nitrogen-terminated surface leads to one nitrogen-derived and one aluminum-derived dangling bond per surface unit cell. The branch originating in the dangling bonds of the adsorbed aluminum atoms (Al in Fig. 9) has an energy of approximately 3 eV. This is about 2 eV lower than the energy of the corresponding state on the cation-terminated surface, reflecting the larger electronegativity of the nitrogen bonding partners. The doubly occupied dangling-bond state of the nitrogen atom not involved in the adsorption (indicated by N) appears slightly above the projected bulk valence bands. The nitrogen-aluminum bonding states are below the valence-band maximum and are not displayed in Fig. 9.

In the case of hydrogen adsorption, no surface state is prominent in the gap. The hydrogen-nitrogen bonds are significantly lower in energy than the valence-band edge. The dangling-bond state related to those surface atoms not bonded to hydrogen is close to the valence-band maximum.

VI. CONCLUSION

By means of *ab initio* tight-binding molecular-dynamics simulations, we have performed extensive calculations to determine energetically stable structures for the (0001) surfaces of GaN and AlN. In the absence of hydrogen, the lowest-energy configurations for the anion- and cation-terminated surfaces of both compounds are the vacancy complex and the vacancy, as can be seen from Figs. 4 and 5. Only under metal-rich growth conditions is the adsorption of a group-III atom on the T_4 position on the cation-terminated surface slightly more favorable than the vacancy. Compared to these lowest-energy structures, the surface energies are 20.1 and 21.3 eV per $p(2\times2)$ unit cell for GaN and AlN if both sides of the crystal films are terminated by ideal surfaces. The large energy difference compared with the vacancy structures, and from all other geometries discussed in Sec. IV, elucidates the instability of the unreconstructed surfaces, and clearly shows that the polarity of the hexagonal surfaces of these materials can be efficiently eliminated by a change of stoichiometry in the topmost layers.

All reconstruction geometries investigated for the the anion- and cation-terminated (0001) surfaces of wurtzite-phase AlN and GaN obey the autocompensation principle. This has been verified by a close inspection of the electronic states of the most stable geometries. Autocompensation requires the entire depopulation of the cation-derived dangling bonds, and a complete occupation of the broken bonds of the anions on the surface to guarantee a semiconducting behavior of the surfaces. This is achieved by the creation of new

dangling bonds through the introduction of vacancies or the adsorption of group-III atoms, group-V atoms, or hydrogen atoms, which reduce the number of dangling bonds.

The presence of hydrogen has an important influence on the growth of the group-III nitrides. Our calculations show that the adsorption of $\frac{3}{4}$ ML of hydrogen leads to stable $p(2\times2)$ configurations on the anion- as well as cation-terminated surfaces. Chemisorption of hydrogen and nitrogen followed by the decomposition of ammonia results in surface structures which are significantly lower in total energy compared to corresponding systems that combine hydrogen free surfaces, whose energies are summarized in Figs. 4 and 5, with free ammonia molecules in vacuum. In the case of the anion-terminated surface, the $\frac{3}{4}$-ML hydrogen adsorption system is lower in energy by 5.1 eV (5.4 eV) for GaN (AlN) compared to a configuration that comprises the nitrogen-vacancy reconstruction and free ammonia molecules. This agrees with the time-of flight scattering and recoiling spectra recorded by Sung *et al.*[1] who examined MOCVD-grown GaN, cleaned by cycles of sputtering and annealing in ultrahigh vacuum. The spectra always showed the presence of hydrogen when sharp $p(1\times1)$ LEED patterns were resolved, indicating an atomically flat nitrogen-terminated surface that is stabilized by the chemisorption of hydrogen.

For all reconstruction geometries considered, we observe an excess of electronic charge in the outermost bilayer on the cation-terminated surface, and a depletion of electronic charge on the opposing anion-terminated side of the crystal films. The appearance and magnitude of such charge accumulation can be explained in terms of Harrison's electron-counting model,[48] taking into account the polarity of the group-III nitrides. For bulk GaN, we obtain a charge transfer of 0.45 electrons from gallium to nitrogen, as indicated by the occupation numbers of the atomic orbitals employed in our calculations [Eq. (1)]. In the case of wurtzite-phase AlN, the computed charge transfer from aluminum to nitrogen amounts to 0.56. If no further charge is transferred, an atomically flat surface will result in an average gradient of the electrostatic potential that corresponds to $\frac{1}{4}$ of the charge in the outermost layer (also compare Fig. 3 of Ref. 48). To compensate for the associated electric field, a charge of the opposite sign and equal in magnitude has to be incorporated into the surface. Analyzing the electronic charge of the vacancy or adatom structures investigated in Sec. IV shows that these configurations are indeed characterized by the exact amount of excess charge necessary to eliminate the electric field arising from the surface polarity. The numbers are 0.45 and 0.56 electrons per $p(2\times2)$ unit cell for GaN and AlN.

Similar to the case for the zinc-blende-compound analogs,[49,50] the cation-terminated surfaces of GaN and AlN are stabilized by the formation of vacancies which introduce three anion-derived dangling bonds replacing one of four cation-derived dangling bonds per unit cell. Accumulation of electronic charge is achieved by occupying the energetically favorable dangling bonds of the anions. In addition to vacancy structures, adatom configurations are able to stabilize the cation-terminated surfaces of AlN and GaN. Especially under metal-rich growth conditions, the chemisorption of group-III atoms is favorable. The creation of electronic charge excess by chemisorption can be explained in the following way: the three dangling bonds which are involved in the chemisorption have to be occupied by a total of six electrons through the formation of the chemical bonds. While three electrons are provided by the adsorbed atom, a total of less than three electrons comes from the four dangling bonds in the $p(2\times2)$ unit cell, because of the polarity of the material. Hence an excess charge which is directly related to the polarity is necessary to obtain complete occupation of the bonding orbitals between the substrate and the adsorbed atom.

In contrast to the zinc-blende compounds, for which the adsorption of trimers has been observed on the anion-terminated surface,[51,52] the most stable geometries obtained for the surfaces of GaN and AlN are the vacancy and the vacancy complex, respectively. The creation of a nitrogen vacancy replaces anion-dangling bonds by a larger number of cation-derived dangling bonds which have to be empty. This guarantees a depletion of electronic charge and thus a neutralization of the polarity of the $(000\bar{1})$ surfaces of AlN and GaN. Among all adsorption geometries, the chemisorption of group-III atoms on the hollow site has the lowest energy. However, the vacancy structures are more favorable. An exception is the adsorption of $\frac{3}{4}$ ML of hydrogen, which yields configurations on both the anion- and cation-terminated surfaces with significantly lower energies. For the adsorption on the nitrogen-terminated surface, more than five electrons are provided by the anion-derived dangling bonds, reflecting the polarity of the material. Three electrons stem from the adsorbed hydrogen. Since only a total of eight electrons can be incorporated into the three hydrogen-nitrogen bonds and into the remaining nitrogen dangling bond per $p(2\times2)$ unit cell, charge depletion on the anion-terminated side is necessary.

In summary, all stable surface structures considered here for the hexagonal surfaces of wurtzite-phase GaN and AlN are characterized by two important principles: (i) autocompensation, and (ii) a related depletion or accumulation of electronic charge. According to the principle of autocompensation, only the energetically more favorable anion-derived dangling bonds are occupied, while the incorporation of electronic charge into cation-derived dangling bonds has to be avoided. Whether complete autocompensation can be achieved or not is dependent on the number of anion- and cation-derived dangling bonds prominent in the respective reconstruction and on the number of electrons. The number of electrons occupying the dangling bonds is influenced by charge depletion or accumulation in the surface region. For a complete compensation of polarization-related electric fields in the slab, an excess charge equal to the cation-anion charge transfer in the bulk is necessary per $p(2\times2)$ unit cell on the cation-terminated side. The same magnitude of charge depletion is necessary on the anion-terminated surface.

After this work was completed, we became aware of two other theoretical investigations for the (0001) surfaces of wurtzite-phase AlN and GaN. In Ref. 57, total-energy differences between various surface geometries considered for AlN(0001) and AlN$(000\bar{1})$ were determined by means of plane-wave calculations. In Ref. 58, experimental results from scanning-tunneling microscopy and reflection high-energy electron diffraction, and theoretical results based on

the plane-wave method, are summarized for the (0001) and $(000\bar{1})$ surfaces of GaN. The surface structures investigated in Refs. 57 and 58 include the geometries considered in our computations, as well as some other configurations giving metallic surface bands. Our surface energies agree with the findings of the plane-wave calculations. Only small differences occur for reconstruction geometries having nearly the same energy. In addition to the theoretical investigations of Refs. 57 and 58, experimental data from angle-resolved photoemission spectroscopy[59] were published after the submission of our work. In the experiments of Refs. 59, a flat electronic surface band with an energy close to the valence-band maximum was observed for the GaN(0001) surface. Its symmetry indicates that the state is of sp_z character, consistent with a dangling-bond state. For the cation H_3 adsorption configuration of the AlN(0001) surface [and similarly for GaN(0001)], our computations give a nitrogen-derived dangling-bond state slightly above the projected bulk valence bands, in good agreement with the experimental findings.

ACKNOWLEDGMENTS

This work was supported by the Alexander von Humboldt Foundation through a *Feodor-Lynen-Forschungsstipendium*, the National Science Foundation (Grant No. DMR-9632635 and Grant No. DMR-9510182), and the Office of Naval Research (Grant No. ONR-94-1883-01 Amd).

[1] M. M. Sung, J. Ahn, V. Bykov, J. W. Rabalais, D. D. Koleske, and A. E. Wickenden, Phys. Rev. B **54**, 14 652 (1996).
[2] F. A. Ponce, C. G. Van de Walle, and J. E. Northrup, Phys. Rev. B **53**, 7473 (1996).
[3] S. Strite and H. Morkoç, J. Vac. Sci. Technol. B **10**, 1237 (1992).
[4] S. Strite, in *Festkörperprobleme/Advances in Solid State Physics*, edited by R. Helbig (Vieweg, Braunschweig, 1995), Vol. 34, p. 79.
[5] P. Hacke, G. Feuillet, H. Okumura, and S. Yoshida, Appl. Phys. Lett. **69**, 2507 (1996).
[6] S. Nakamura, M. Senoh, and T. Mukai, J. Appl. Phys. **30**, L1708 (1991).
[7] S. Nakamura, M. Senoh, S. Nagahama, N. Iwasa, T. Yamada, T. Matsushita, H. Kiyoku, and Y. Sugimoto, Jpn. J. Appl. Phys. **35**, L74 (1996).
[8] V. M. Torres, M. Stevens, J. L. Edwards, D. J. Smith, R. B. Doak, and I. S. T. Tsong, Appl. Phys. Lett. **71**, 1365 (1997).
[9] V. M. Bermudez, R. Kaplan, M. A. Khan, and J. N. Kuznia, Phys. Rev. B **48**, 2436 (1993).
[10] M. A. Khan, J. N. Kaznia, D. T. Ohlson, and R. Kaplan, J. Appl. Phys. **73**, 3108 (1993).
[11] K. Iwata, H. Asahi, S. J. Ju, K. Asami, H. Fujita, M. Fushida, and S. Gonda, Jpn. J. Appl. Phys. **35**, L289 (1996).
[12] M. E. Lin, S. Strite, A. Agarwal, A. Salvador, G. L. Zhou, N. Teraguchi, A. Rockett, and H. Morcoç, Appl. Phys. Lett. **62**, 702 (1993).
[13] W. C. Hughes, W. H. Rowland, Jr., M. A. L. Johnson, S. Fujita, J. W. Cook, Jr., J. F. Schetzina, J. Ren, and J. A. Edmond, J. Vac. Sci. Technol. B **13**, 1571 (1995).
[14] W. E. Packard, J. D. Dow, K. Doverspike, R. Kaplan, and R. Nicolaides, J. Mater. Res. **12**, 646 (1997); W. E. Packard, J. D. Dow, R. Nicolaides, K. Doverspike, and R. Kaplan, Superlattices Microstruct. **20**, 145 (1996).
[15] M. Buongiorno Nardelli, K. Rapcewicz, and J. Bernholc, Bull. Am. Phys. Soc. **42**, 170 (1997).
[16] R. B. Capaz, H. Lim, and J. D. Joannopoulos, Phys. Rev. B **51**, 17 755 (1995).
[17] R. Di Felice, J. E. Northrup, and J. Neugebauer, Phys. Rev. B **54**, R17 351 (1996).
[18] S. Y. Ren and J. D. Dow, Appl. Phys. Lett. **69**, 251 (1996).
[19] L. K. Teles, L. M. R. Scolfaro, R. Enderlein, J. R. Leite, A. Josiek, D. Schikora, and K. Lischka, J. Appl. Phys. **80**, 6322 (1996); J. Yamauchi, M. Tsukada, S. Watanabe, and O. Sugino, Phys. Rev. B **54**, 5586 (1996); K. Osuch and W. S. Verwoerd, Surf. Sci. **345**, 75 (1995).
[20] O. F. Sankey and D. J. Niklewski, Phys. Rev. B **40**, 3979 (1989).
[21] O. F. Sankey, D. A. Drabold, and G. B. Adams, Bull. Am. Phys. Soc. **36**, 924 (1991).
[22] A. A. Demkov, J. Ortega, O. F. Sankey, and M. P. Grumbach, Phys. Rev. B **52**, 1618 (1995).
[23] J. Ortega, J. P. Lewis, and O. F. Sankey, Phys. Rev. B **50**, 10 516 (1994).
[24] G. B. Adams, J. B. Page, O. F. Sankey, and M. O'Keeffe, Phys. Rev. B **50**, 17 471 (1994).
[25] G. B. Adams and O. F. Sankey, J. Vac. Sci. Technol. A **10**, 2046 (1991).
[26] D. R. Alfonso, D. A. Drabold, and S. E. Ulloa, Phys. Rev. B **51**, 1989 (1995).
[27] A. F. Wright and J. S. Nelson, Phys. Rev. B **50**, 2159 (1994).
[28] I. Gorczyka, N. E. Christensen, E. L. Peltzer y Blancá, and C. O. Rodriguez, Phys. Rev. B **51**, 11 936 (1995).
[29] K. Miwa and A. Fukumoto, Phys. Rev. B **48**, 7897 (1993).
[30] J. E. Northrup and J. Neugebauer, Phys. Rev. B **53**, R10 477 (1996).
[31] K. Kádas, S. Alvarez, E. Ruiz, and P. Alemany, Phys. Rev. B **53**, 4933 (1996).
[32] P. Hohenberg and W. Kohn, Phys. Rev. **136**, B864 (1964).
[33] W. Kohn and L. J. Sham, Phys. Rev. **140**, A1133 (1965).
[34] D. M. Ceperley and B. J. Alder, Phys. Rev. Lett. **45**, 566 (1980).
[35] J. P. Perdew and A. Zunger, Phys. Rev. B **23**, 5048 (1981).
[36] D. R. Hamann, M. Schlüter, and C. Chiang, Phys. Rev. Lett. **43**, 1494 (1979).
[37] J. Harris, Phys. Rev. B **31**, 1770 (1985).
[38] D. G. Anderson, J. Assoc. Comput. Mach. **12**, 547 (1965).
[39] M. Finnis, J. Phys. Condens. Matter **2**, 331 (1990).
[40] H. J. Monkhorst and J. D. Pack, Phys. Rev. B **13**, 5188 (1976).
[41] H. Schulz and K. H. Thiemann, Solid State Commun. **23**, 815 (1977).
[42] K. Tsubouchi, K. Sugai, and N. Mikoshiba, *1981 Ultrasonics Symposium Proceedings* (IEEE, New York, 1981), Vol. 1.
[43] P. Perlin, A. Polian, and T. Suski, Phys. Rev. B **47**, 2874 (1993).
[44] A. Tabata, R. Enderlein, J. R. Leite, S. W. da Silva, J. C. Galzerani, D. Shikora, M. Kloidt, and K. Lischka, J. Appl. Phys. **79**, 4137 (1996).
[45] L. E. McNeil, M. Grimsditch, and R. H. French, J. Am. Ceram. Soc. **76**, 1132 (1983).

[46] F. Bernardini, V. Fiorentini, and D. Vanderbilt, in *III-V Nitrides*, edited by F. A. Ponce, T. D. Moustakas, I. Akasaki, and B. A. Monemar, MRS Symposia Proceedings No. 449 (Materials Research Society, Pittsburgh, 1996).
[47] C. B. Duke, Scanning Microsc. **8**, 753 (1994).
[48] W. A. Harrison, J. Vac. Sci. Technol. **16**, 1492 (1979).
[49] K. W. Haberern and M. D. Pashley, Phys. Rev. B **41**, 3226 (1990).
[50] L. Ö. Olsson, L. Ilver, J. Kanski, P. O. Nilsson, C. B. M. Andersson, U. O. Karlsson, and M. C. Håkansson, Phys. Rev. B **53**, 4734 (1996).
[51] D. K. Biegelsen, R. D. Bringans, J. E. Northrup, and L.-E. Schwartz, Phys. Rev. Lett. **65**, 452 (1990).
[52] C. B. M. Andersson, U. O. Karlsson, M. C. Håkansson, L. Ö. Olsson, L. Ilver, P. O. Nilsson, J. Kanski, and P. E. S. Persson, Phys. Rev. B **54**, 1833 (1996).
[53] G.-X. Qian, R. M. Martin, and D. J. Chadi, Phys. Rev. B **38**, 7649 (1988).
[54] P. Boguslawski, E. L. Briggs, and J. Bernholc, Phys. Rev. B **51**, 17 255 (1995).
[55] D. J. Chadi, Phys. Rev. Lett. **57**, 102 (1986).
[56] E. Kaxiras, Y. Bar-Yam, D. J. Joannopoulos, and K. C. Pandey, Phys. Rev. Lett. **57**, 106 (1986).
[57] J. E. Northrup, R. Di Felice, and J. Neugebauer, Phys. Rev. B **55**, 13 878 (1997).
[58] A. R. Smith, R. M. Feenstra, D. W. Greve, J. Neugebauer, and J. E. Northrup, Phys. Rev. Lett. **79**, 3934 (1997).
[59] S. S. Dhesi, C. B. Stagarescu, K. E. Smith, D. Doppalapudi, R. Singh, and T. D. Moustakas, Phys. Rev. B **56**, 10 271 (1997).